Near-field Scanning Optical Microscopy (NSOM) study of alkyl-substituted polyfluorene films: The affect of alkyl substituent length on nanoscale polymer ordering and cluster formation.

Julie Teetsov,* David A. Vanden Bout

Department of Chemistry, University of Texas at Austin, Austin, TX, 78712, U.S.A.

SUMMARY: Pristine and Annealed 170 nm films of the stiff-chain polyfluorene, bearing two hexyl (**1**) or dodecyl (**2**) groups at the 9 position were studied using Near-field Scanning Optical Microscopy (NSOM). NSOM images reveal two distinct types of nanoscale film morphology: clusters and long-range order (LRO). Dual polarization and dual wavelength fluorescence collection schemes are combined with the use of simple image math provide both qualitative and quantitative characterization. In pristine films, shorter alkyl substituents (**1**) reduce the solubility of the polyfluorene in the spinning solution used for spin-coating films which leads to the formation of 50–150 nm clusters which are not present in films made from **2**. Clusters can be removed by annealing as a function of time. Polarization shows the clusters are amorphous with fluorescence from both intra and inter-polymer species. The second variety of nanoscale ordering, LRO, is characterized by regions of polarized emission in the polymer films. This polarization can be quantified with an anisotropy value and is barely present in pristine films of **1** but increases dramatically upon annealing to induce a liquid crystalline phase transition. Pristine films of **2** have larger anisotropy values than pristine films of **1**, due to longer alkyl-substituent-induced ordering during the spin-coating procedure, but films of **2** have only a slight increase in their anisotropy value upon annealing. Both intra and inter-polymer emitting species are distributed homogeneously throughout both pristine and annealed films within the resolution of our microscope (40–70 nm).

Introduction

There is great interest in the structure-property relationships of stiff-chain fluorescent polymer films because of their potential use in a wide variety of electro-optic devices. A stiff chain affords a variety of processing advantages for ordering polymers over large areas in thin films.[1] Several studies have used stiff chain fully conjugated polymers to create polarized light-emitting films,[2] nano-ribbons,[3] and aggregated polymer species with enhanced fluorescence quantum yields.[4,5] In dilute solutions, with

* Present Address: General Electric Corporate Research & Development, K1-1C10, P.O. Box 8, Schenectady, NY 12301

 CCC 1022-1360/00/$ 17.50+.50/0

minimal inter-polymer interactions, stiff-chain polymer fluorescence is well characterized, with predictable fluorescence spectra and quantum yields. In going from dilute solutions to thin films, a variety of new intra and inter-polymer species are formed which introduce new electronic ground and excited state complexes.[6] As a result of the multi-variant nature of 1) the formation of inter and intra-polymer species and 2) the mechanisms responsible for the fluorescence of these species, the ability to control spectral properties and maximize quantum yields in polymer films has not yet been achieved.

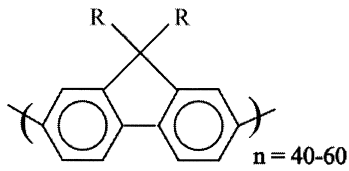

1) R = *n*-C_6H_{13}; **2**) R = *n*-$C_{12}H_{25}$

Inter-polymer complexes affect film ground state absorption, fluorescence spectra and fluorescence quantum yield. Inter-polymer interactions result from enhanced polymer packing and the nature of this packing is affected by both the polymer's intra-polymer conformational changes and inter-polymer interactions. Two of the major factors affecting stiff-chain homo-polymer packing are 1) processing conditions[7-11] and 2) the nature of the substituent added to the polymer backbone.[12] These substituents are either straight or branched chain alkyl groups[13,14] or functionalized to afford the desired solubility[12] or dielectric properties.[15,16]

In this study we characterize the affect of alkyl substituents on nanoscale self-ordering in 170 nm films made via spin-coating stiff chain, liquid crystalline polyfluorene solutions, with either two hexyl (**1**) or dodecyl (**2**) groups at the 9 position. We use Near-field scanning optical microscopy (NSOM) to resolve and quantifying two types of nanoscale ordering: 1) clusters and 2) long range order (LRO) in both pristine and annealed films of **1** and **2**. Previous qualitative studies using conventional polarized light microscopy[12] demonstrated microscale nematic liquid crystalline ordering in annealed films of **1** and **2**, but not in pristine films, which were characterized as amorphous.[17] With the order of magnitude greater resolution in NSOM than in conventional microscopy, while we are still not able to resolve intra-polymer conformational changes

in the polymer backbone that contribute to the polymer's ability to pack, we are able to resolve and *quantify* the degree of inter-polymer packing. We detect alkyl-substituent-induced LRO in pristine films of **1** and **2**. We determine that shorter dihexyl substituents afford the formation of highly ordered lamellae with an overall film anisotropy value six times as great as didodecyl polyfluorene films which can be linked to an increase in low energy film fluorescence. We determine the spin-coating concentration below which clusters are no longer resolved via NSOM in films of **1** and **2** in toluene solutions.

Near-Field Scanning Optical Microscopy is a scanning probe microscopies technique which takes advantage of simultaneously collecting topographic and fluorescence images by scanning with a force feedback mechanism in the near-field with a fiber optic probe. The excitation light is forced through the probe's sub-wavelength aperture onto the sample to create an evanescent field that contains the high spatial frequency information whose lateral extent is confined by the size of the aperture. An NSOM image is formed by collecting fluorescence in the far-field while scanning the aperture over the sample and while keeping the sample tip separation constant and within the near-field. The resolution of the fluorescence collected in the far-field is defined primarily by the size of the aperture of the near-field probe, 50–100 nm, an order of magnitude better than conventional light microscopy whose resolution is limited by diffraction.[18-20] NSOM has been used to probe a variety of organic, inorganic, and biological systems.[21] We extend the contrast in NSOM by dual polarization and dual wavelength collection. By simultaneous collection at dual polarizations we are able to quantify the degree of ordering through an anisotropy calculation image.[22] We then measure the variance in this anisotropy value by repeated scanning of numerous samples. There have been relatively few studies that have microscopically characterized conjugated polymer film morphology.[8,23-26] Schartz et al. use atomic force microscopy to study films of MEH-PPV, but their results are of surface topography without the fluorescence information provided by using NSOM. Blatchford et al. and Buratto et al. use NSOM to qualitatively characterize films of PPV. Being able to assign a quantitative nanoscale anisotropy value to polymer films is a great step forward for NSOM materials characterization.

Polyfluorene is an ideal polymer for taking advantage of both of these new quantitative NSOM techniques of fluorescence anisotropy measurement and spectral filtering. Previous single photon counting studies[12] have shown that the fluorescence of **1** and **2** in dilute solution arise from a single 500 ps emitting species, which we refer to as

intra-polymer emission.[12] As thin films, the fluorescence spectra of **1** and **2** red-shifts from solution, and there is an increase in low energy emission. While the high energy fluorescence (440 nm) remains single exponential as in solution, the new low energy fluorescence (500–600 nm) is comprised of the solution like emission and two new long-lived fluorescing species (> 1–3 ns). These long-lived species are thought to arise from inter-polymer species formed in the ground or the excited state.[12] The contribution from these inter-polymer species increases dramatically upon annealing films to induce liquid crystalline self-ordering, and the temperature required for the liquid crystalline transition increases with decreasing alkyl substituent length. Interestingly, the percent contribution of the inter-polymer species is much greater in annealed films of **1** than in annealed films of **2**, while in pristine films, the order is reversed with greater inter-polymer emitting species in films of **2** than films of **1**. Previous studies on have provided extensive information of bulk photophysical properties of dialkylpolyfluorenes as dilute solutions and as ordered thin films.[5,12,13,15,27] Both ground state aggregate and excimer formation have been shown to either raise[5] or lower[28] the fluorescence quantum yield, respectively, depending on alkyl substituent length and processing conditions. These studies raise new questions as to the nature of the inter-polymer interaction in polyfluorenes films. By using NSOM to characterize the affect of alkyl substituent length on the degree of nanoscale ordering and correlating this with the subsequent bulk fluorescent properties, we determine how polymer film morphology can be modified to afford the desired fluorescent properties through synthetic tuning of the the stiff-chain polymer substituent.

Experimental

Simultaneous Collection: Schemes 1 & 2. Near-field and topographic images were collected with a modified Topometrix Aurora NSOM. Fig. 1 shows a diagram of the instrument and the two unique collection schemes. Excitation wavelengths of 390 and 437 nm were achieved with a Spectra Physics Tsunami Ti:Sapphire Laser focused through a BBO doubling crystal. The polarization of the excitation light was adjusted with a combination of half and quarter-wave plates prior to focusing into the near-field probe. Probes were fabricated from a single mode optical fiber whose tapered end was coated with aluminum.[19] The probe and sample were kept within 7 ± 0.25 nm by tuning

fork[29,30] shear-force mechanism. The collection objective was focused onto the fluorescence excited by the probe and this distance was kept constant during the scan

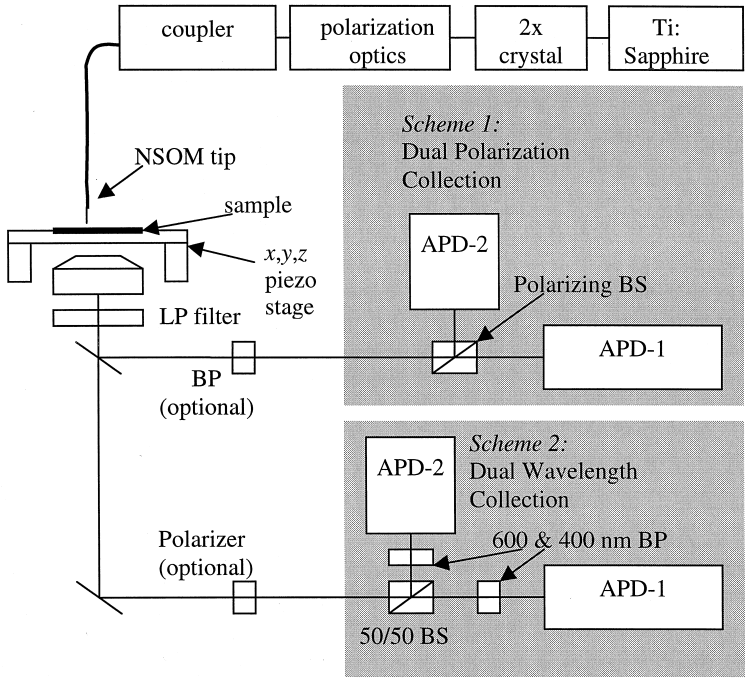

Fig. 1 Diagram of the NSOM instrument showing the two schemes used for dual image collection. Scheme 1: two imges are collected simultaneously at two polarizations. Scheme 2: two images are collected simultaneously at two wavelengths. APD, BS, LP, BP refer to avalanche photo diode, beam splitter, and low pass and band pass filters.[22]

while the sample was moved in the *X,Y* and *Z* directions with a piezo-electrically driven sample stage. Schemes 1 & 2 in Fig. 1 represent simultaneous imaging of either two polarizations or two wavelengths of emission by passing the fluorescence through a polarizing or non-polarizing beam splitter, respectively. The fluorescence photons were focused onto two avalanche photo diodes (APDs) during scanning and two fluorescence images were recorded simultaneously along with a topographic image. Band pass filters (440 and 600 nm) or a combination of long pass (530 nm) and short pass (485 nm) filters were used to provide spectral filtering either before the beam splitter as in Scheme 1, or immediately before the APDs as in Scheme 2. The sample was raster scanned over 2 μm areas at 2.5 μm/s with a resolution of 200 pixels to give 10 nm pixel sizes with 10 ms photon counting per pixel.

Thin Film Preparation. Thin films were prepared by spin coating (Specialty Coating Systems Inc.) 2 wt% polymer and toluene solutions onto glass cover slips. Film thickness was maintained at 170 nm by spinning at 3000 rpm for 30 s. Because **1** is less soluble than **2**, it required heating to produce a clear violet solution prior to spin coating.

Results and Discussion

Bulk Absorbance and Fluorescence Spectra. The absorbance and fluorescence spectra of pristine and annealed films of **1** and **2** are shown in Fig. 2a,b, respectively. The absorbance spectra of **2** shows a maximum at 390 nm, and upon annealing, a new peak appears as a shoulder at around 437 nm. This peak has been previously reported as being due to polymer aggregates.[31] Pristine and annealed films of **1** (not shown) show a similar trend in absorbance spectra to pristine and annealed films of **2**.

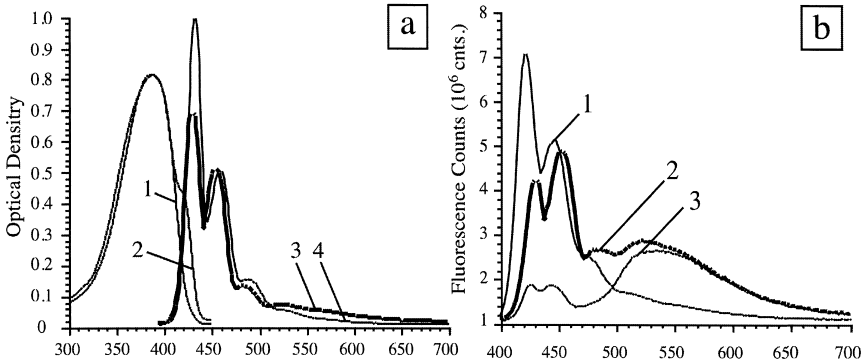

Fig. 2. a) absorbance and fluorescence spectra of **2** as pristine (1,4) and annealed (2,3) 170 nm films; b) fluorescence spectra of **1** as pristine (1), and annealed for 2 hrs (2) and 12 hrs (3) films; λ_{excite}= 390 nm.

The fluorescence spectra of an annealed film of **2** has a slight decrease in high energy emission (due in part to self-absorption), and a slight increase in low energy emission as compared to a pristine film of **2** (Fig. 2a). Slight differences in the sample thickness, crystallinity, and angle of collection hinder the ability to compare absolute fluorescence intensities. Instead, we compare the relative intensity of the second (448-458 nm) intra-polymer fluorescence peak (not affected by self-absorption) to the broad and featureless inter-polymer fluorescence peak (centered at approx. 550 nm). The pristine films of **1** and **2** have very similar relative ratios of intra to inter-polymer emitting species. There is a larger decrease in the relative ratio of the intra to inter-polymer emission in annealed films of **1** as compared to **2** (Fig. 1b). After further

annealing (12 hrs), the relative ratio shifts further in favor of the inter-polymer species in films of **1** (spectra 3 of Fig 1b). After annealing, the intra-polymer peak shifts from 455 to 458 nm in films of **2**, but remains at 448 nm in films of **1**. Annealed films of **1** exposed to atmosphere for approx. 6 weeks show a slight red-shift in the fluorescence peak from 448 to 454 nm and a slight increase in low energy emission, while aged annealed films of **2** and pristine films of **1** and **2** show minimal spectral shifts with aging. Therefore, films of **2** reach a plateau in their film fluorescence spectra after 2 hrs annealing, while further annealing or aging is required for films of **1**. Furthermore, in pristine films, the differences in the length of the alkyl substituents do not affect fluorescence behavior while in annealed films, shorter alkyl substituents lead to greater inter-polymer fluorescence.

Insoluble Clusters. NSOM topographic images of pristine films show no clusters in 170 nm films of **2** and 25–75 nm wide and 15–30 nm high clusters observed in films of **1**. The longer alkyl substituents of **2** versus **1** better solublize the polymer in the toluene solution used for spin coating, where the concentration of the spinning solution is used to determine the thickness of the film (with other parameters such as spin speed held constant). In previous studies of pristine 250 nm thick films of **1** and **2**, larger 50–150 nm clusters are observed and occur with greater frequency in films of **1** than films of **2**.[22] In this study, where thickness is reduced to 170 nm, there are no clusters observed in pristine films of **2**, and the clusters observed in films of **1** are smaller in size than those observed in previous studies on thicker films. A further decrease in the concentration of the spinning solution, to make 70 nm films, removes all clusters from pristine films of **1**. Therefore, these clusters are most likely due to insoluble aggregates forming in the polymer solution prior to spinning. Annealing films of **1** for two hours at the liquid crystalline phase transition temperature does not reduce the size or frequency of the cluster, but longer annealing times (12 hours) reduces the frequency of the clusters dramatically as they appear to "melt" into the surrounding polymer's lamellae structures.

In previous studies on thicker pristine films[22] of **1** and **2**, the fluorescence associated with the topographic clusters was lower in intensity, and favored 600 over 440 nm emission. Similar cluster-correlated fluorescence was not readily observed in the thinner films used in this study. The correlation of the thickness of the clusters and the decrease in fluorescence intensity at higher energies, suggest that the cluster correlated fluorescence results from polymer self-absorption. This is observed in Fig. 2a where the

absorption spectra broadens with greater inter-polymer interaction which in turn lowers the intensity of higher energy fluorescence. NSOM images taken at orthogonal polarizations show that the cluster-correlated fluorescence in the thicker films is not polarized, because the features have the same intensity in both images. Therefore, there are greater inter-polymer interactions in the cluster regions, but not in any particular order as seen in the LRO discussed in the following section. Clusters have also been reported in films of MEH-PPV[8] using AFM where topographic images reveal clusters of similar dimensions which form as a result of processing and solubility conditions. Schwartz et al. state that the clusters may be a manifestation of smaller scale aggregation beyond the resolution of the AFM, and that these aggregated species may be responsible for the reduced fluorescence efficiency of devices

Long-Range Order. Long-range order (LRO) is observed in both topographic and fluorescence NSOM images of pristine films of **2** as shown in Fig. 3. The LRO in the topographic NSOM image (Fig. 3a) is relatively smooth with a min to max vertical topography of 13 nm. Lateral features are between 50–200 nm in width and length. After annealing the film (Fig. 4a), the topography does not change significantly; the min

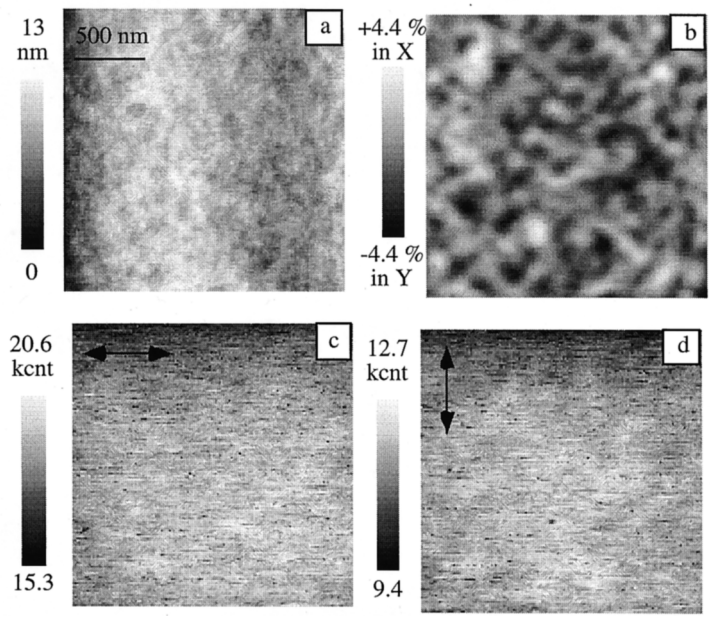

Fig. 3. NSOM images of 2 x 2 μm scans of *pristine* 170 nm films of **2**; a) topography; b) anisotropy image calculated from images 3c,d; c,d) fluorescence images excited with circularly polarized 400 nm light and collected simultaneously at orthogonal polarizations at all wavelengths.

to max vertical topography doubles, but the overall LRO patterns remain the same. There appears to be no correlation between topographical LRO features and the intensity or polarization of fluorescence in the corresponding fluorescence NSOM images.

Fluorescence NSOM images are simultaneously collected at orthogonal polarizations using Scheme 1 shown in Fig. 1. The fluorescence images shown here were collected at all wavelengths, but images were also collected at specific wavelengths corresponding to intra versus inter-polymer emitting species.[22] Pristine films of **2** have 50–200 nm regions of LRO which are identified as ordered, because the dark regions of less fluorescence correspond directly with bright regions of more fluorescence in the image collected at the orthogonal polarization and visa versa (Figs. 3c,d). After annealing, the fluorescence LRO in the films of **2** (Figs. 4c,d) maintains the size and

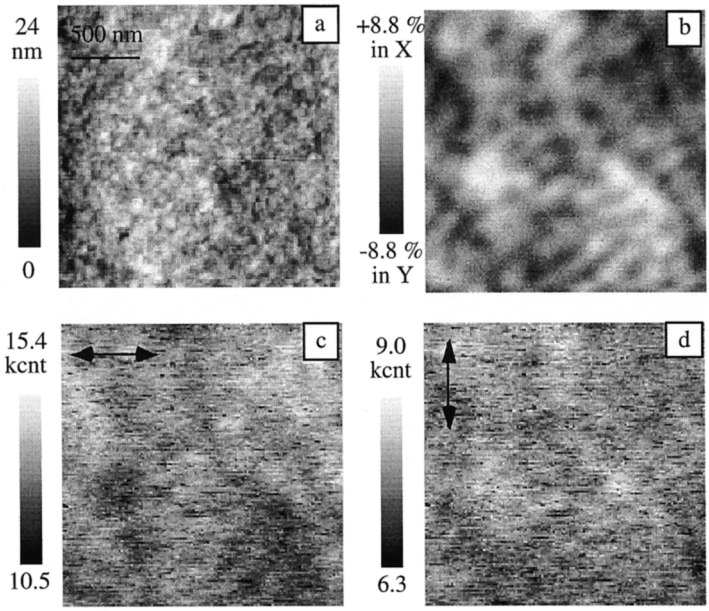

Fig. 4. NSOM images of 2 x 2 μm scans of *annealed* 170 nm films of **2**; a) topography; b) anisotropy image calculated from images 3c,d; c,d) fluorescence images excited with circularly polarized 400 nm light and collected simultaneously at orthogonal polarizations at all wavelengths.

shape of its continuous pattern, but the percent contrast between light and dark regions increases from approx. 26% in the pristine film to 32%, indicative of greater polymer packing. In order to enhance contrast and provide a quantitative measure of ordering, we calculate an anisotropy image shown in Fig. 3b and 4b for pristine and annealed films of **2**, respectively. To calculate anisotropy, the two normalized orthogonal fluorescence

images are subtracted from each other, and this difference image is divided by an addition image of the same two raw fluorescence images. The resulting anisotropy image reflects the direction of ordering, where light regions are oriented parallel to the scan direction (*X*) and dark regions are oriented perpendicular to the scan direction (*Y*). The gray in the middle of the scale represents regions oriented at 45° to the collection polarization. There are no regions that are completely polarized in one direction (anisotropy = 100%), but the LRO varies smoothly throughout the film with a maximum value of ±4.4% in pristine films of **2** (Fig. 3b) and ±8.8% in annealed films of **2** (Fig. 4b). Further annealing past 2 hrs does not alter the anisotropy value.

The topographical LRO in pristine films of **1** is less apparent than in pristine films of **2** (Fig. 5a); frequent clusters preclude proper tracing of the tip to reveal the possible presence of subtle topography. In annealed films of **1** (Fig. 5b), clusters remain and rope-like two dimensional "lamellae" form as a result of annealing for 2hrs. After annealing for 12 hrs, the system reaches an equilibrium state where the majority of clusters have "melted" into the surrounding lamellae. After 2 hrs, the lamellae length vary between 100–500 nm while 12 hrs of annealing produces longer 500 nm to 1 μm lamellae. The width of the lamellae remains constant irregardless of annealing time and the distribution of this width matches that of the polymer's molecular weight of 40–70 nm (as previously determined via GPC).[12] The fluorescence NSOM images collected at orthogonal polarizations show a minimum in fluorescence when the collection polarization is aligned with the lamellae's long axis and a maximum in fluorescence when the collection polarization is aligned perpendicular to the lamellae's long axis.[32] The fluorescence dipole is aligned with the polymer axis, and so in addition to the width of the lamellae, this fluorescence polarization data indicates that the lamellae are composed of polymers aligned perpendicular to the lamellae's long axis. The ability to measure a distribution of the widths of these lamellae can provide useful information about the stiff-chain polymer's molecular weight distribution. This has recently been demonstrated for end-functionalized poly(*para*-phenyleneethynylene)s (PPEs), where the molecular weight, which is often difficult to determine experimentally for stiff-chain polymers, was determined statistically via numerous AFM measurements of the width of polymer "ribbons" forming on flat crystalline substrates.[3]

Fluorescence NSOM images of pristine and annealed films of **1** are shown in Figs. 5c and 5d. The LRO in the pristine film of **1** is ±4% which is similar to that of the pristine film of **2** (±4.4%). The LRO is significantly larger in the annealed film of **1** than

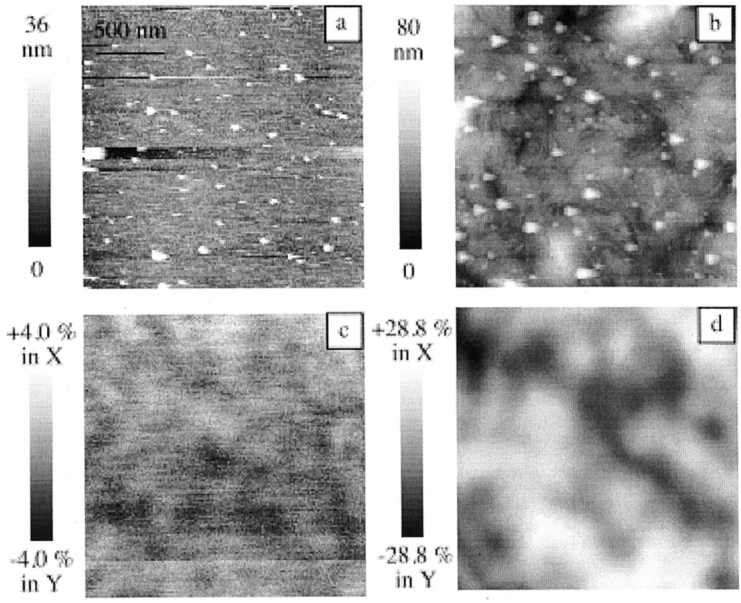

Fig. 5. NSOM images of 2 x 2 μm scans of 170 nm films of **1**; a) topography of pristine and annealed films, respectively; b) anisotropy calculation images of corresponding pristine (c) and annealed (d) films of **1**.

in the annealed film of **2** due to the increased order and the formation of lamellae. The LRO increases upon annealing from 2 to 12 hrs. After 2 hrs annealing the fluorescence anisotropy increases from ±4% as a pristine film to ±28%, and after 12 hrs the anisotropy approx. doubles to between ±45–50%.[32] Therefore, shorter alkyl substituents allow for greater polymer packing via liquid crystalline self-ordering as measured by a larger anisotropy values for annealed films of **1** as compared to films of **2**. The greater packing on a molecular scale enhanced by shorter alkyl substituents may explain the formation of the lamellae seen only in the annealed films of **1** and not the annealed films of **2**. Conversely, the formation of lamellae, somehow favored by the shorter alkyl substituents, may be responsible for the greater molecular scale packing as measured by our anisotropy image.

The positive correlation between the relative ratio of intra to inter-polymer bulk fluorescence and nanoscale LRO indicates that NSOM fluorescence anisotropy values

can be used to determine the quality of polymer packing in films and will affect bulk fluorescence. Previous studies on the bulk fluorescence lifetimes of thicker (250 nm) films of **1** and **2** also correlate with NSOM anisotropy values as summarized in Table 1.[12]

Table 1. Comparison of Average NSOM Fluorescence Anisotropy with Bulk Fluorescence Lifetimes and Quantum Yields

	NSOM[a]		*Bulk Film Fluorescence*[b]	
	Fluorescence Anisotropy (± %)	Topography (± nm)	Interpolymer Species (%)	Fluorescence Quantum Yield (%)
1–Pristine	5.2 ± 2.5	21 ± 8	6	15.5
1–Annealed	30.2 ± 2.0	101 ± 34	46	10.0
2–Pristine	6.5 ± 2.0	15 ± 4	12	15.5
2–Annealed	7.8 ± 1.8	20 ± 3	23	13.5

[a]170 nm film[32)]
[b]250 nm film[22)]

An increase in the inter-polymer species with a subsequent decrease in fluorescence quantum yield parallels an increase in anisotropy in films of **1**, and not in films of **2**. The reason for this is that there there are several varieties of inter-polymer interactions, some of which are not measured by the anisotropy calculation. The average topographical and anisotropy values for films of **1** and **2** along with standard deviations are also summarized in Table 1. The average values are calculated from 2–3 batches of samples where numerous scans were taken of each sample. The values of the specific images shown in this paper reflect these average values.

Conclusions

The spatial dimensions and anisotropy of nanoscale LRO may be affected by polymer chain length in addition to the length of the alkyl substituent. Because the degree of polymerization is the same for **1** and **2**, we can assume that the differences observed in LRO between films of **1** and **2** are controlled by the length of the alkyl substituent. The fact that LRO is present in pristine films of **1** and **2** prior to annealing implies that LRO begins during the spin-coating procedure. Because there is a slightly larger anisotropy value associated with *pristine* films of **2** than films of **1**, longer alkyl substitutents increase the polymer's ability to pack as a pristine film. A comparison of fluorescence NSOM images of *annealed* films of **1** and **2** illustrates that shorter alkyl substituents allow for greater packing. While the anisotropy doubles for annealed films

of **2**, it increases by a factor of ten for annealed films of **1**. In addition, NSOM topography coupled with fluorescence polarization imaging indicate that lamellae formed in annealed films of **1** are composed of polymer's aligned perpendicular to the length of the lamellae. As a result of a correlative study of NSOM and bulk measurements, the red-shifted fluorescence spectra and enhanced low energy emission, with a greater contribution from long-lived fluorescence species, can be partially attributed to nanscale LRO. Future work will

Acknowledgement

We gratefully acknowledge Drs. Edward P. Woo and Michael Inbasekaran at The Dow Chemical Company for the polymer samples used in this study. Drs. Don O'Conner and Marye Anne Fox are thanked for their support during the collection fluorescence lifetime and quantum yield data. D.A.V.B. gratefully acknowledges the Camille and Henry Dreyfus Foundation for a New Faculty Award. This work was supported by the NSF (Grant 9875313) and the Robert A. Welch Foundation (Grant F-1377). The authors also thank Dr. Stefan Kaemmer and other individuals at Thermomicroscopes for their support of our research and many useful discussions concerning NSOM.

References

1. Balauff, M. *Macromol.* **1986**, *19*, 1366-74.
2. Palmans, A. R. A.; Eglin, M.; Montali, A.; Weder, C.; Smith, P. *Chem. Mater.* **2000**, *12*, 472-480.
3. Samori, P.; Francke, V.; Mullen, K.; Rabe, J. P. *Chem. Eur. J.* **1999**, *5*, 2312-2317.
4. Jenekhe, S. A.; Chen, X. L. *Science* **1998**, *279*, 1903-1907.
5. Grell, M.; Bradley, D. D. C.; Ungar, G.; Hill, J.; Whitehead, K. S. *Macromol.* **1999**, *32*, 5810-5817.
6. Conwell, E. *Trends Polym. Sci.* **1997**, *5*, 218-222.
7. Yang, Y.; Shi, Y.; Liu, J. *J. Appl. Phys.* **2000**, *87*, 4254-4263.
8. Nguyen, T.; Martini, I. B.; Liu, J.; Schwartz, B. J. *J. Phys. Chem. B* **2000**, *104*, 237-255.
9. Nguyen, T.; Kwong, R. C.; Thompson, M. E.; Schwartz, B. J. *Appl. Phys. Lett.* **2000**, *76*, 2454-2456.
10. Bradley, D. D. C.; Grell, M.; Long, X.; Mellor, H.; Grice, A. *SPIE* **1997**, *3145*, 254-259.
11. Grell, M.; Bradley, D. D. C.; Inbasekaran, M.; Woo, E. P. *Adv. Mater.* **1997**, *9*, 798-802.
12. Teetsov, J.; Fox, M. A. *J. Mater. Chem.* **1999**, *9*, 2117-2122.
13. Lee, J.; Klarner, G.; Chen, J. P.; Scott, J. C.; Miller, R. D. *Proc. SPIE Int. Soc. Opt. Eng.* **1999**, *3623*, 2-12.
14. Bernius, M.; Inbasekaran, M.; Woo, E. P.; Wu, W.; Wujkowski, L. *Proc. SPIE-*

Int. Soc. Opt. Eng. **1999**, *3621*, 93-102.
15. Pei, Q.; Yang, Y. *J. Am. Chem. Soc.* **1996**, *118*, 7416-7417.
16. Yang, Y.; Pei, Q.; Heeger, A. J. *J Appl Phys* **1996**, *79*, 934-939.
17. Redecker, M.; Bradley, D. D. C.; Inbasekaran, M.; Woo, E. P. *Appl. Phys. Lett.* **1999**, *74*, 1400-1402.
18. Betzig, E.; Trautman, J. K. *Science* **1992**, *257*, 189-195.
19. Betzig, E.; Trautman, J. K.; Harris, T. D.; Weiner, J. S.; Kostelak, R. L. *Science* **1991**, *251*, 1468-1470.
20. Paesler, M. A.; Moyer, P. J. *Near-Field Optics Theory, Instrumentation and Applications*; Wiley: New York, 1996.
21. Dunn, R. C. *Chem. Rev.* **1999**, *99*, 2891-2927.
22. Teetsov, J.; Bout, D. A. V. *J. Phys. Chem. B.* **2000**, *104,* 9378-9387.
23. Blatchford, J. W.; Gustafson, T. L.; Epstein, A. J.; Higgins, D. A.; Vanden Bout, D. A.; Kerimo, J.; Barbara, P. A. *Phys. Rev. B* **1996**, *R3683*.
24. DeAro, J. A.; Weston, K. D.; Buratto, S. K.; Lemmer, U. *Chem. Phys. Lett.* **1997**, *277*, 532-538.
25. DeAro, J. A.; Moses, D.; Buratto, S. K. *Appl. Phys. Lett.* **1999**, *75*, 3814-3816.
26. Credo, G. M.; Lowman, G. M.; DeAro, J. A.; Carson, P. J.; Winn, D. L.; Buratto, S. K. *J. Chem. Phys.* **2000**, *112*, 7864-7872.
27. Fukuda, M.; Sawda, K.; Yoshino, K. *J Polym Sci, Part A: Polym, Chem.* **1993**, *31*, 2465-2471.
28. Bliznyuk, V. N.; Carter, S. A.; Scott, J. C.; Klarner, G.; Miller, R. D.; Miller, D. C. *Macromol.* **1999**, *32*, 361-369.
29. Karrai, K.; Grober, R. D. *Ultramicroscopy* **1995**, *61*, 197-205.
30. Ruiter, A. G. T.; Veerman, J. A.; van der Werf, K. O.; van Hulst, N. F. *Appl. Phys. Lett.* **1997**, *71*, 28-30.
31. Grell, M.; Bradley, D. D. C.; Long, X.; Chamberlain, T.; Inbasekaran, M.; Woo, E. P.; Soliman, M. *Acta. Polym.* **1998**, *49*, 439-444.
32. Teetsov, J.; Bout, D. A. V. *submitted to JACS*.